Metallobiochemistry of ultratrace levels of bismuth in the rat

II. Interaction of $^{205+206}Bi^{3+}$ with tissue, intracellular and molecular components

Enrico Sabbioni[1,3], Flavia Groppi[2,3], Mario Di Gioacchino[1,4], Claudia Petrarca[1,5], Simone Manenti[2,3]*

1. Center for Advanced Studies and Technology (C.A.S.T.), "G. d'Annunzio" University of Chieti-Pescara, Via Luigi Polacchi 11, Chieti, I-66100, Italy

2. Department of Physics, Università Degli Studi di Milano, Via Celoria 16, Milano, I-20133, Italy

3. LASA, Department of Physics, Università Degli Studi di Milano and INFN-Milano, Via F.lli Cervi 201, Segrate (MI) I-20090, Italy

4. Institute of Clinical Immunotherapy and Advanced Biological Treatments, Piazza Pierangeli 1, Pescara; Rectorate of Leonardo da Vinci Telematic University; Largo San Rocco 11 Torrevecchia Teatina, CH, Italy

5. Department of Medicine and Aging Sciences, "G. d'Annunzio" University of Chieti-Pescara, via Luigi Polacchi 11, Chieti, I-66100, Italy

*Corresponding author: simone.manenti@mi.infn.it

Abstract

Background: Knowledge on Bi metabolism in laboratory animals refers to studies at “extreme” exposures, i.e. pharmacologically relevant high-doses (mg/kg b.w.) in relation to its medical use, or infinitesimal doses (pg/kg b.w.) concerning radiobiology protection and radiotherapeutic purposes. There are no specific studies on metabolic patterns of environmental exposure doses (ultratrace level, µg/kg b.w.), becoming in this context Bi a “heavy metal fallen into oblivion”. We previously reported the results of the metabolic fate of ultratrace levels of Bi in the blood of rats

[1]. In reference to the same study here we report the results of the retention and tissue binding of Bi with intracellular and molecular components.

Methods: Animals were intraperitoneally injected with 0.8 µg Bi/kg b.w. as $^{205+206}Bi(NO)_3$, alone or in combination with ^{59}Fe for the radiolabeling of iron proteins. The use of $^{205+206}Bi$ radiotracer allowed the determination of Bi down to pg/fg in biological fluids, tissues, subcellular fractions, and biochemical components isolated by differential centrifugation, size exclusion chromatography, solvent extraction, precipitation, immunoprecipitation and dialysis.

Main findings: At 24h post injection the kidney contained by far the highest Bi concentration (10 ng/g wt.w.) followed by the thymus, spleen, liver, thyroid, trachea, femur, lung, adrenal gland, stomach, duodenum and pancreas (0.1 to 1.3 ng/g wt.w.). Brain and testis showed smaller but consistently significant concentrations of the element (0.03 ng/g wt.w). Urine was the predominant route of excretion. Intracellularly, liver, kidney, spleen, testis and brain cytosols displayed the highest percentages (35% to 58%) of Bi of homogenates. Liver and testis nuclei were the organelles with the highest Bi content (24% and 27%). However, when the recovered Bi of the liver was recorded as percent of total recovered Bi divided by percent of total recovered protein the lysosomes showed the highest relative specific activity than in other fractions. In the brain subcellular fractions Bi was incorporated by neuro-structures with the protein and not lipidic fraction of the myelin retaining 18% of Bi of the total homogenate. After the liver intra-subcellular fractionation: (i) 65% of the nuclear Bi was associated with the protein fraction of the nuclear membranes and 35% with the bulk chromatin bound to non-histone and DNA fractions; (ii) about 50% of the mitochondrial Bi was associated with inner and outer membranes being the other half recovered in the intramitochondrial matrix; (iii) in microsomes Bi showed a high affinity (close to 90%) for the membranous components (rough and smooth membranes); (iv) In the liver cytosol three pools of Bi-binding proteins (molecular size > 300 kDa, 70 kDa and 10 kDa) were observed

with ferritin and metallothionein–like protein identified as Bi-binding biomolecules. Three similar protein pools were also observed in the kidney cytosol. However, the amount of Bi, calculated in percent of the total cytosolic Bi, were significantly different compared to the corresponding pools of the liver cytosol.

Conclusions: At the best of our knowledge the present paper represents the first *in vivo* study, on the basis of an environmental toxicology approach, aiming at describing retention and binding of Bi in the rat at tissue, intracellular and molecular levels.

Keywords

Bismuth; Radioisotopes; Environmental toxicology; Metabolic pattern; Rat tissues

1. Introduction

Bismuth (Bi) is a naturally occurring pnictogen element belonging to the group of heavy metals. It is traditionally regarded as the element with the heaviest stable isotope, though this is not strictly true due to the discovery of the primordial nuclide bismuth-209 that has the longest known half-life of any radionuclide ($T_{1/2}$=1.9 ×10^{19} y, more than a billion times the age of the universe) [2]. Although its position in the periodic table is in the midst of toxic heavy metals (lead, antimony, polonium) Bi and its compounds have a low environmental impact and good biocompatibility for humans and other mammalians, being referred as a "green element" [3]. The use of Bi is growing very fast in the last decades. In 2018 approximately 16 000 tons of refinery Bi were produced worldwide, with China leading with ca. 79.9% of the world's total production [4]. In industry, Bi compounds and alloys have widespread commercial applications such as in the manufacture of semiconductors [5], in the production of grease, chemicals, catalysts, shot bullets, fire sprinkler

systems, solders, thermoelectric materials, fishing sinkers [6] and in magnetic levitation (Maglev) trains [7]. In cosmetics Bi-salts are used in formulations marketed as “mineral makeup” (i.e. lipstick, nail polish, eye shadows and facial powders [8], and in hair dyes to add color and to deodorize [9]. Bi, with over 200 y history in medicine [10], is one of the medicinal drugs listed in Pharmacopoeias as highly effective antimicrobial agent in treating intestinal disorders, particularly peptic gastritis and ulceration, and venereal diseases [8]. Moreover, it has potential activities against viruses and tumors [4]. Bi has found applications in catheters reducing bacterial colonization [11] and in diagnostic and surgical procedures [12]. Although occupational exposure to Bi may occur in the manufacture of cosmetics, industrial chemicals and pharmaceuticals [8], most cases of poisoning occurred following accidental or deliberate over-dosage with Bi-containing drugs that allowed induction of encephalopathy, nephropathy, gingivostomatitis, osteoarthropathy, and colitis [13]. Moreover, in the last decade the bursting advent of the era of nanomaterials has opened extraordinary perspectives about industrial and biomedical use of Bi in the innovative form of nanoparticles (BiNP) [14]. In industry, BiNP such as chalcogenide (Bi_2O_3, Bi_2S_3 ,Bi_2Se_3, Bi_2Te_3), oxalide (BiOCl, BiOBr, BiOI), and Bi_2WO_6, $(BiO)_2CO_3$, $BiVO_4$, $BiPO_4$, BiFeO , Bi_2MoO_6, BisBAL (bismuth dimercaptopropanol nanoparticles) are excellent candidates for many applications that include preparation of nanostructures, photocatalysts, solid oxide fuel cells, gas sensors, catalysts for oxidation of hydrocarbons, catalytic performance for reduction, water purification and photovoltaic [15, 16, 17]. Moreover, Bi-based NP have many potential medicinal properties, such as antibacterial, antibiofilm, fungicidal, antiviral activity [18, 19, 20], thermo-chemotherapy [21], imaging [22] and radiosensitizing agent for X-ray radiation therapy [23]. However, the expected wide placing on the market of such innovative Bi-based nanomaterials poses serious concerns about their toxicity. This because the toxicological response of nanomaterials depends on factors (high surface / volume ratio and "nano" physical size) not

normally relevant in the toxicology of the corresponding macromaterials [24]. Unfortunately, the issue of the BiNP toxicity is in its infancy and until now few and contrasting results are reported about the toxicity of Bi at the nanoscale level [25]. BiNP induced low toxicity both *in vitro* in Hela cells and *in vivo* in mice [26]. Absence of damage to genomic DNA was reported for blood cells exposed to BisBAL [27]. In contrast, DNA damage, apoptosis, and oxidative stress effects have been induced by BiNP in four cell lines [25] while cytotoxic effects in a dose dependent manner were observed in Balb/3T3 cells exposed to colloidal suspensions of BiNP [28]. Moreover, (Bi_2Se_3)NP induced long term immune-toxic effects over lungs of mice, raising serious concern about their *in vivo* hazardous effects [29].Then, the toxicity of BiNP remains a controversial issue, questioning whether Bi is really a "green element" [30]. In this scenario the evaluation of the nanotoxicity mechanisms of BiNP is an urgent need before their placing on the market. Nanotoxicology studies on metal-based NPs have shown that they can diffuse into tissues, internalized into cells, penetrating into cell organelles, releasing metal ions in such compartments [31]. This may happen also for the BiNP that may generate intracellular Bi ions whose metabolic fate and toxicity need to be evaluated. In this context, the knowledge of the metabolic patterns of ultratrace levels of Bi in experimental animal models is of paramount importance [1]. To fill this gap, we have undertaken a study of the metabolic patterns of ultratrace levels of $^{205+206}Bi^{3+}$ in the rat. The results of the first part of the study (distribution of ^{206}Bi among blood components) have been reported elsewhere [1]. The present paper concerns the second part of the study related to the distribution of $^{205+206}Bi$ in tissues, subcellular fractions with the identification of cellular Bi-binding components.

2. Materials and methods

2.1. Chemicals and reagents

Chemicals and reagents used have been listed elsewhere [1]. Moreover, Sepharose 6B was supplied by Pharmacia, Uppsala, Sweden; rabbit anti-horse spleen ferritin from Serva, Heidelber, Germany.

2.2. Radiotracers and radioactive counting

No-Carrier-Added (NCA) $^{205+206}$Bi radiotracers ($t_{1/2}$= 15.3 d and 6.24 d, respectively) were prepared by proton activation of metallic Pb, radiochemically separated and the characteristics of the final solution for biochemical purpose determined as described elsewhere [1]. The final $^{205+206}$Bi solution (hereinafter simply referred as ^{206}Bi) had the following characteristics: radioactive concentration: 2 mCi (37 Mbq)/mL; radiochemical purity: > 99% (by paper chromatography in butanol-water thiocyanic solution); radionuclidic purity: > 99% (by ^{206}Bi decay and gamma spectra); chemical impurities: < 1 µg/mL (by INAA, AAS and ICPMS); specific radioactivity: 14 µCi (0.52 Mbq)/ng Bi as determined by pre-concentration on Chelex 100 column [36], elution with 2M HNO_3 followed by ICPMS [37]; final chemical form: isotonic solution of $Bi(NO)_3$ pH 5.6, sterilized by filtration (recovery of ^{206}Bi > 88%).

$^{59}FeCl_3$ (specific activity 4.5 µCi (0.167 MBq)/ µg Fe) was purchased from the Radiochemical Centre, Amersham, UK.

Complementary and alternative radioactive counting techniques used were: (i) integral γ-counting to measure ^{206}Bi alone by a Wizard 3 Gamma Counter apparatus (Perkin Elmer, Life Sciences) equipped with a well-type 3.15" x 3" NaI(Tl) size crystal; (ii) computer-based γ-ray spectrometry using a HPGe detector (EG&G Ortec Int,GA,USA) for the simultaneous measurement of ^{206}Bi and ^{59}Fe [1].

2.3. Animals and treatment

Rats were male Sprague-Dawley rats (250 ± 20 g, Harlan Nossan, Correzzana. Italy). Housing conditions, experimental procedures, exposure, and treatment of animals were reported elsewhere [1]. They were in strict accordance with the European Community regulations [32]. Briefly, in a first step five animals were intraperitoneally (i.p.) injected with a single dose of Bi (0.8 µg Bi/kg b.w. as $Bi(NO)_3$ plus 46.8 µCi (1.73 MBq) of ^{206}Bi /rat in the same chemical form). In a second step, three rats were individually i.p. injected with 52 µCi (1.92 MBq) of ^{206}Bi $(NO)_3$ (0.89 µg Bi/kg b.w.) together with 1.2 µg Fe^{3+} as chloride plus 10 µCi (0.37 MBq) of ^{59}Fe in the same chemical form.

2.4. Excretion and tissue retention

Fecal pellets and urine were collected every 6 h. Twenty-four hours after dosing rats were anaesthetized with Nembutal (40 mg/kg b.w.) and sacrificed by cardiac puncture. Blood was collected by heparinized syringes and centrifuged at 2 500 g for 15 min to separate plasma and red blood cells (RBC) and the two compartments fractionated to study the distribution of Bi among blood components [1]. The animals were dissected, the body tissues sampled, cleaned by removing the visible fat, washed with ice-cold 0.9% saline solution, mopped dry and weighed. Liver and kidney were perfused. Hair and skin were sampled from a small area on the abdomen. The fat sampled was abdominal fat. The contents of the stomach and intestines were extruded and were not included with the intestinal tissue for analysis. Kidney was dissected into outer cortex and inner medulla. The femur, after a thorough cleaning of muscle residues and connective tissue, was cut into 5 parts (two epiphysis and three from the diaphysis). All tissues and sub-regions were analyzed for the ^{206}Bi content.

2.5. Subcellular distribution

Liver, kidney, spleen, testis and brain were homogenized in 0.25 mol/l sucrose, 10 mM sodium cacodylate-HCl buffer, pH= 7.2 and the crude subcellular fractions prepared by differential centrifugation by a TL-100 ultracentrifuge, Beckmann Instrument, Palo Alto, CA (700 g for 10 min to sediment nuclear fraction; 9 000 g for 15 min to yield the mitochondrial fraction; 30 000 g for 25 min to sediment the lysosomal fraction, 105 000 g for 110 min to yield microsomes and organelle-free cytosol) [1]. The brain was fractionated into seven intracellular fractions as reported in [33], using a cacodylate buffer for homogenization. All subcellular fractions were washed once with the same buffer and the washing added to the following centrifugation steps. The liver and kidney crude subcellular fractions were further re-suspended in sucrose cacodylate buffer and further purified by centrifugation of: (i) the nuclear pellets on “dense solution” (2 M sucrose, 70 mM KCl [34]); (ii) the mitochondrial pellets on a sucrose gradient (1.8-2.0 M) [25]; (iii) the microsomal fraction at 105 000 g for 90 min . All subcellular fractions were counted for the ^{206}Bi content. The relative purity of the liver subcellular fractions was assessed by specific marker enzymes and the nuclear marker DNA according to standard procedures. Recovery was followed by determining the DNA [36] or the total activity of the marker enzyme of each fraction compared to the homogenate. The enzyme markers assayed were: cytochrome c oxidase [37], aryl sulphatase A+B [38], glucose-6-phosphatase [39] and lactate dehydrogenase [40] as markers of mitochondrial, lysosomal, microsomal and cytosol fractions, respectively. Proteins were determined according to Bradford [41] with bovine serum albumin as standard. The distribution of different enzymes in the purified liver subcellular fractions was expressed graphically as De Duve’s plot [42].

2.6. Liver subcellular sub-fractionation

2.6.1. Nuclear sub-fractions were: nuclear membranes and its lipid and protein sub-fractions; bulk chromatin and its DNA and histone protein sub-fractions. They were isolated according to Franke [34] with some modifications concerning: (i) the isolation of histone proteins (extraction from chromatin at 4^{o}C with 20 vol. of ethanol/ 1.25 M HCl (4:1 v/v), centrifugation (15 000 g, 15min), addition of acetone to the supernatant to precipitate the histone proteins, centrifugation, followed by three washings); (ii) the separation of DNA (further step of purification by precipitating the re-suspended 198 000 g pellet by 35% isopropanol and 0.5 M salt).

2.6.2. Mitochondrial sub-fractions were: heavy and light subfractions (corresponding to inner and outer mitochondrial membranes, respectively) and mitochondrial soluble matrix subfraction. They were isolated as described elsewhere [35].

2.6.3. Microsomal sub-fractions were: smooth membranes, light and heavy rough membranes, soluble fraction and free polysomes. They were obtained according to the Tata's procedure [43].

2.6.4. Liver and kidney cytosolic proteins were fractionated by SEC on Sephadex G-75 column (2.5 cm x 100 cm) previously equilibrated with 10 mM cacodylate buffer, pH 7.2, using the same buffer as eluent [44]. The collected fractions of the eluate were analyzed for the absorbance at 280 nm and the ^{206}Bi content. In addition, aliquot of the whole liver and kidney cytosols were heated at 80^{0}C for 2 min, rapidly cooled in ice and the heat-coagulated proteins removed by centrifugation (15 000 g, 10 min). Thereafter the supernatant was submitted to SEC as described above.

2.6.5. Separation of lipids from the nuclear membranes, membranous mitochondrial and microsomal components and myelin fraction was carried according to Folch's method [45].

2.7. Isolation of [^{206}Bi + ^{59}Fe]-double labelled ferritin

The ^{206}Bi+^{59}Fe-liver cytosol, prepared as described above in the Section 2.6.4. was heated at 80^0C and stirring for 10 min, ferritin being resistant to denaturation. [46]. The heat-coagulated proteins were removed by centrifugation (20 000 g, 10 min) resulting in a relative enrichment of ferritin in the soluble fraction. The latter was submitted to SEC on Sepharose 6B (2.5 cm x 60 cm) previously equilibrated with cacodilate buffer, pH 7.2 and pre-calibrated with a kit of proteins with known molecular weight. Protein of the eluate was monitored at 280 nm and the [^{206}Bi+^{59}Fe] profiles obtained by γ-ray spectrometry. The [^{206}Bi +^{59}Fe] peaks emerging from the column were pooled, concentrated by ultrafiltration and assayed with anti-horse spleen ferritin, an antibody cross-reacting with rat ferritin [47]. Immunoprecipitation was carried out as described elsewhere [46]. ^{206}Bi and ^{59}Fe were measured in the immunoprecipitate after centrifugation (3 000 g, 10 min).

2.8. Dialysis experiments

Visking semi-permeable membrane tubing (MW cut off: 12- 14 kDa) were used for extensive dialysis of ^{206}Bi-containing liver, kidney and brain subcellular fractions and their components (three changes of 2 L of 10 mM cacodylate buffer, pH 7.2 alone or containing chelating agents (EDTA, DMSA or citrate) as well as against 10 mM acetate buffer, pH 5.0). The ^{206}Bi of the dialyzed sample was measured in the membrane tubing before and after dialysis [1].

3. Results

3.1. Tissue retention and excretion

Table1. Distribution of Bi in tissues of rats after 24 h of i.p. injection of 0.8 µg Bi/kg b.w. as $^{206}Bi(NO)_3$ [a].

Tissue	Bi content	
	%dose/g tissue	ng Bi/g tissue
Kidney	11.2 ± 2.13	10.2 ± 1.6
Cortex	~ 10.3	-
Medulla	~ 0.9	-

Adrenal gland	0.004 ± 0.003	0.16 ± 0.09
Spleen	0.34 ± 0.16	1.3 ± 0.6
Liver	3.34 ± 1.31	0.75 ± 0.25
Pancreas	0.11 ± 0.03	0.13 ± 0.04
Lung	0.07 ± 0.02	0.17 ± 0.02
Testis	0.03 ± 0.01	0.03 ± 0.04
Heart	0.010 ± 0.005	0.021± 0.007
Femur	0.064 ± 0.023	0.17 ± 0.04
Epiphysis[b]	0.046 ± 0.018	-
Diaphysis[b]	0.018 ± 0.009	-
Rib[c]	0.05 ± 0.03	0.11± 0.06
Brain	0.03 ± 0.01	0.03 ± 0.01
Cerebellum	0.033 ± 0.005	0.16± 0.03
Thymus	0.38 ± 0.18	1.50 ± 0.65
Thyroid	0.006 ± 0.004	0.48 ± 0.25
Trachea	0.005 ± 0.003	0.22 ± 0.15
Duodenum	0.042 ± 0.03	0.14 ± 0.09
Stomach	0.09 ± 0.03	0.16 ± 0.55
Intestine small	0.17 ± 0.07	0.036 ± 0.008
Intestine large	0.11 ± 0.09	0.07 ± 0.05
Fat[c]	0.003 ± 0.002	0.012 ± 0.008
Muscle[c]	0.02 ± 0.01	0.016 ± 0.007
Skin[c]	0.011 ± 0.006	0.012 ± 0.005
Hair[c]	0.008 ± 0.006	0.02 ± 0.01
Blood	0.09 ±0.02	0.18 ± 0.05

a: mean of 5 animals ± SD

b: 78% of the total ^{206}Bi of the femur recovered in the epiphyses; 12% in the diaphysis with concentrations declining from the epiphyses to the center of the bone

c: % dose/g tissue. Assuming that the total size of muscle, fat , skin, bone accounted for approx 45.5%, 7%, 18% and 10% of the body weight [48, 49, 50] the estimated total amount of Bi in such whole tissues were: 1.8 ng, 0.2 ng, 0.5 ng and 3.7 ng, respectively

Table 1 shows the distribution of Bi in tissues of rats 24 h after i.p. injection of 0.8 µg Bi/kg b.w. as $^{206}Bi(NO)_3$. Bi was recovered in all tissues. The kidney was by far the tissue with the highest amount of the element both in terms of percentage of the dose administered and concentration (10 ng Bi/g wt.w.). Following, to a lesser extent, the thymus, spleen, liver, thyroid, trachea, femur, lung, adrenal gland, stomach, duodenum and pancreas (concentrations from 0.1 to 1.3 ng Bi/g wt.w.). A ratio of the concentration in kidneys to that in liver averaged 13.6. All other tissues had concentrations

lower than 0.1 ng Bi/g tissue. In the femur 78% of Bi was present in the epiphysis and 22% in the three parts of the diaphysis, of which the central segment showed the lowest ^{206}Bi concentration. The elimination of ^{206}Bi in urine and feces is shown in Fig.1. Urine was the main route of excretion with about 12.5% of the dose administered at 24 h post-injection period. The corresponding fecal elimination accounted for the 8% of the Bi injected.

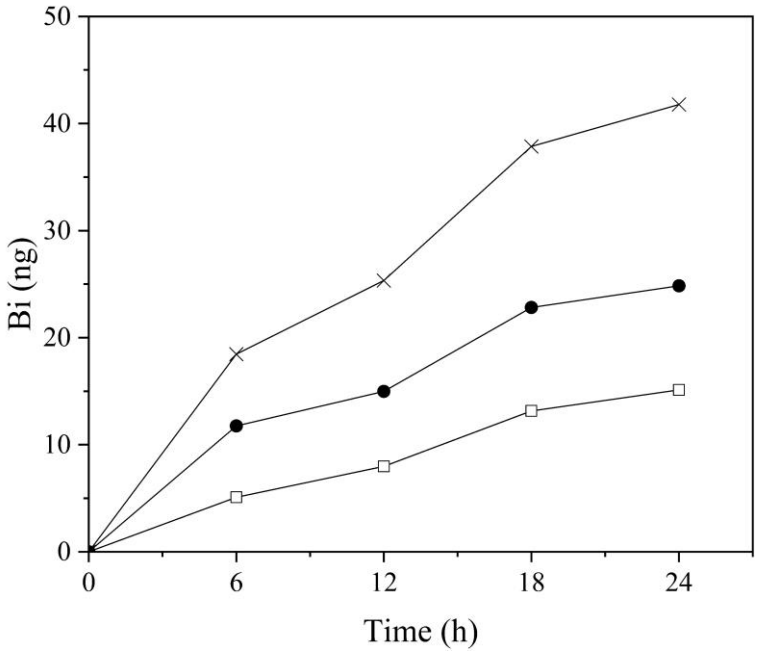

Fig.1 Cumulative excretion pattern of ^{206}Bi in urine and feces of rats 24 h after i.p. injection of 0.8 µg Bi/kg b.w. as $^{206}Bi(NO)_3$. Urine and feces were collected every 6 h. Mean of 5 animals, RSD < 20%. Solid circle: urine; open circle: feces; X: total

3.2. Subcellular distribution

The content of proteins, Bi, DNA, and the activities of enzyme markers in each liver intracellular fraction are shown in Table 2. Plot of the mean relative to specific activity of the enzyme markers of the fractions against the recovered proteins (DeDuve's plot, Fig.2) suggests a good degree of purification of the subcellular fractions achieved over the homogenate.

Table 2. Percentage of total protein, Bi, DNA and marker enzymes in purified liver subcellular fractions of rats after 24 h i.p. injection of 0.8 µg Bi/kg b.w. as $^{206}Bi(NO)_3$[a]

Purified subcellular fraction	Protein	Bi	DNA	Cytochrome oxidase	Aryl sulphatase A+B	Glucose-6 - phosphatase	Lactate dehyrogenase
Nuclei	21 ± 2	23.6 ± 3.4	91 ± 7	10 ± 3	21 ± 1	12 ± 2	6 ± 2
Mitochondria	16 ± 3	15.5 ± 2.6	6 ± 3	69 ± 5	23 ± 3	4 ± 1	3 ± 1
Lysosomes	7 ± 2	18.7 ± 3.0	4 ± 1	7 ± 1	32 ± 4	11 ± 3	4 ± 1
Microsomes	12 ± 1	8.9 ± 1.2	n.d.[b]	3 ± 1	11 ± 2	54 ± 4	7 ± 2
Cytosol	48 ± 4	35.4 ± 2.2	n.d.	n.d.	5 ± 3	5 ± 3	77 ± 5
Total recovery	104 ± 6	102.1 ± 5.8	101 ± 8	89± 6	92 ± 6	86± 6	97± 6

a: mean ± SEM on 5 determinations

b: not detected

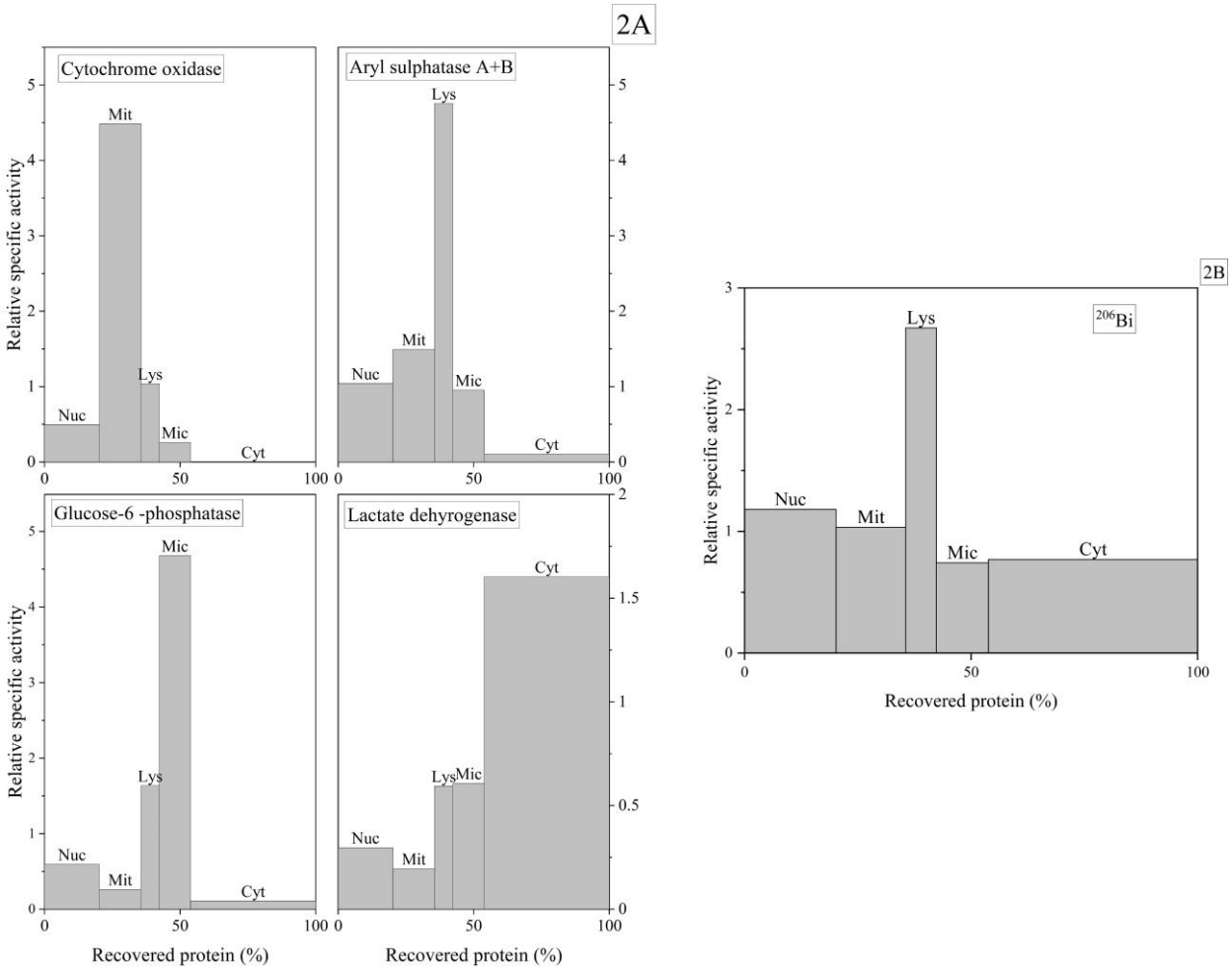

Fig.2 Average intracellular distribution pattern of marker enzymes (**2A**) and ^{206}Bi (**2B**) over subcellular fractions of the liver as obtained by differential centrifugation of the homogenate (cytochrome c oxidase (EC 1.9.3.1); aryl sulphatase (EC 3.1.6.1); glucose-6-phosphatase (EC 3.1.3.9); lactate dehydrogenase (EC 1.1.1.27)). Recoveries were 86-97%. Blocks from left to right represent: nuclear (Nuc), mitochondrial (Mit), lysosomal (Lys), microsomal (Mic) and cytosol (Cyt) fractions. Ordinate scale: relative specific activity of the

enzyme (percentage of total recovered activity/percentage of total recovered protein). Abscissa scale: cumulative percentage of protein.

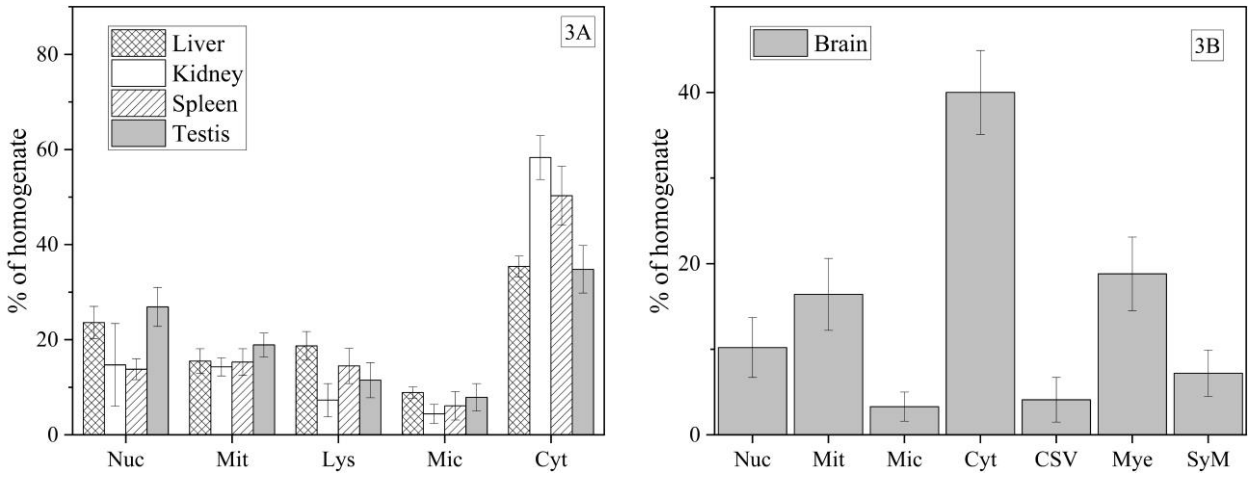

Fig.3 Intracellular distribution of Bi in liver, kidney, spleen, pancreas, testis (**3A**) and brain (**3B**) of rats 24 h after i.p. injection of 0.8 µg Bi/kg b.w. as $^{206}Bi(NO)_3$. The results, expressed as the percentage of the total ^{206}Bi in the homogenate, are the mean of individual tissues (n=5). The subcellular fractions were isolated by differential centrifugation. Crude (spleen, testis, brain) or further purified (liver and kidney) subcellular fractions were counted for the ^{206}Bi radioactivity. Nuc, Mit, Lys, Mic, Cyt: nuclear, mitochondrial, lysosomal, microsomal and cytosol fractions. CSV, Mye, Sy: Crude Synaptic Vesicles, Myelin and Synaptic membranes fractions. For details see Section 2.5.

Fig.3 shows the intracellular distribution of ^{206}Bi, expressed as percentage of the total Bi of the homogenate, in purified (liver and kidney) or crude (spleen, testis and brain) subcellular fractions. In all tissue analyzed the highest percentage of the intracellular ^{206}Bi was recovered in the cytosol, from 35% to 58% in the liver and kidney, respectively. Liver and testis nuclei were the organelles with the highest ^{206}Bi content (24% and 27%, respectively). The presence of ^{206}Bi in mitochondria of all tissues analyzed did not show significant fluctuations, varying from 14.3% (kidney) to 18.9% (testis). In contrast with other tissues the lysosomes of the kidney contained approximately half of Bi compared to the other lysosomal fractions. However, when Bi recovered in the liver subcellular fractions was recorded according to the DeDuve's plot (percent of total recovered Bi divided by percent of total recovered protein) the relative specific activity was higher in the lysosomes than

in other fractions(Fig.2). In the brain subcellular fractions 30% of the Bi was recovered in neuro-structures. Myelin fraction retained 18% of the total brain Bi (Fig.3), essentially bound to proteins, as suggested by: (i) the small amount of ^{206}Bi extracted with lipids that was not considered significant under our experimental conditions (less than 1.7% of the total Bi associated with myelin); (ii) the similar amount of ^{206}Bi removed by dialysis of the Bi-myelin fraction before and after lipid extraction (Table 3).

Table 3. Dialysis of ^{206}Bi-containing liver, kidney and brain intracellular components of rats 24 h after i.p. injection of 0.8 µg Bi/Kg b.w. as $^{206}Bi(NO)_3$ [a]

Intracellular component	^{206}Bi (% of the applied radioactivity retained inside the tubing at the end of dialysis)				
	10mM cacodilate pH 7.2 (Cac)	10mM acetate pH 5.0	Cac+ 1mM EDTA	Cac + 1mM DMSA	Cac + 1mM citrate
LIVER					
Nuclei:					
Nucl. membranes	93.6	13.6	16.6	5.4	14.8
Histone proteins	86.2	9.6	13.5	3.9	n.d.[c]
DNA	93.4	1.4	10.0	4.4	14.2
Mitochondria:					
Outer membranes	88.2	11.5	24.2	4.7	14.8
Outer membranes[b]	89.8	14.6	n.d.	6.3	n.d.
Inner membranes	90.4	10.4	9.9	9.2	13.7
Inner membranes[b]	88.7	13.2	n.d.	8.1	n.d.
Soluble matrix	91.6	1.6	n.d.	4.5	11.6
Lysosomes (whole)	93.8	11.0	16	7.0	n.d.
Microsomes:					
Smooth membranes	87.7	14.7	22.3	7.1	21.0
Heavy rough membranes	93.5	15.5	n.d.	10.4	27.2
Heavy rough membranes[b]	92.5	12.3	n.d.	8.0	n.d.
Light rough membranes	93.4	14.2	21.6	5.1	24
Light rough membranes[b]	94.7	17.8	17.7	n.d.	n.d.
Soluble fraction	90.6	9.5	12.5	7.9	23.3
Cytosol (whole)	94.1	6.4	23.5	8.5	25.4
KIDNEY					
Nuclei	93.6	5.6	n.d.	11.4	25.4
Mitochondria	91.3	11.2	18.4	10.9	17.7
Lysosomes	92.1	8.8	9.3	6.5	n.d.
Microsomes	89.8	13.4	23	8.8	23.7
Cytosol	64.4	12.8	29.6	7.2	18.0
BRAIN					
Nuclear fraction	90.2	4.4	16.5	4.9	13.0

Mitochondria fraction	95.0	8.3	n.d.	7.7	n.d.
Myelin fraction	95.7	9.6	13.8	5.7	14.1
Myelin fraction[b]	94.2	6.7	n.d.	7.2	19.3

a: mean of 3 determinations, RSD: < 25%. In the control ($^{206}Bi^{3+}$ alone in cacodylate and acetate buffers) the applied radioactivity retained in the tubing at the end of the dialysis ranged from 3.1 to 9.0%

b: after lipid extraction. For details see Section 2.6.5.

c: not determined

3.3. Sub-fractionation of subcellular fractions

Fig.4 summarizes the results of the distribution of Bi in the sub-fractions of the purified liver ^{206}Bi-containing nuclei, while Table 4 reports the corresponding results for mitochondria and microsomes.

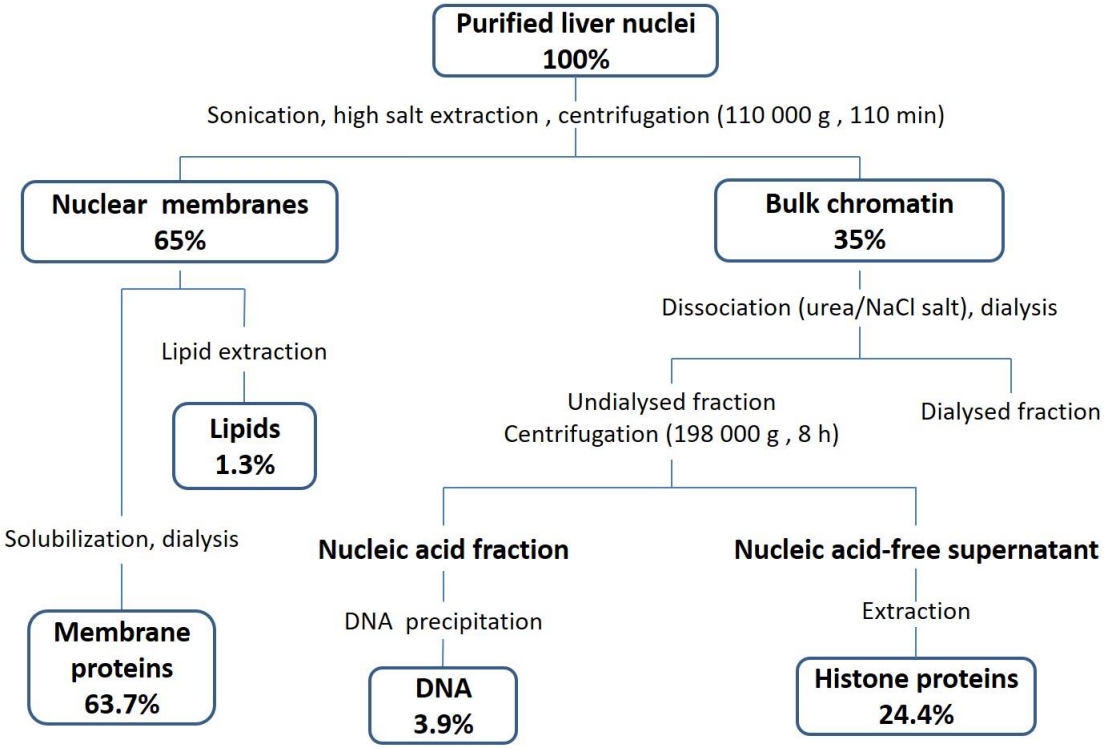

Fig.4 Average intranuclear distribution of Bi in purified rat liver nuclei 24 h after i.p. injection of 0.8 µg Bi/kg b.w. as $^{206}Bi(NO)_3$. Results are expressed in pg Bi/nuclear subfraction. Mean ± RSD (n=3); SD < 18%. The methods of nuclei fractionation are also reported. The DNA purity was assessed by the measurement of the A_{260nm}/A_{280nm} (1.86) and A_{260nm}/A_{230nm} (1.97) ratios. For details see Section 2.6.

Table 4. Average distribution of Bi among the purified liver mitochondrial and microsomal subfractions 24 h after i.p. injection of 0.8 µg Bi/kg b.w. as $^{206}Bi(NO)_3$ [a]

Subcellular fraction / sub-fractions	^{206}Bi recovered in the fraction/subfraction	
	%	pg
Mitochondria:	100	1050
Soluble fraction	52 ± 5	548 ± 11
Light subfraction[b]	11 ± 2	113± 13
Heavy subfraction[c]	37 ± 6	390 ± 9
Heavy subfraction:	100	360
Lipid fraction[d]	< 2	< 8
Light subfraction:	100	98
Lipid fraction[d]	< 1.4	< 1.5
Microsomes:	100	600
Heavy rough membranes	59 ± 6	354 ± 9.2
Smooth membranes	21 ± 3	126 ± 14.5
Light rough membranes	11 ± 3	66 ± 6
Soluble fraction	6 ± 3	36 ± 5
Free polysomes	3 ± 2	18 ± 3
Heavy rough membranes:	100	302
Lipid fraction[d]	1.8	5.4
Light rough membranes:	100	51
Lipid fraction[d]	< 2.5	< 1.3

a: mean of 5 experiments ± SD
b: corresponding to outer membranes
c: corresponding to inner membranes
d: recovered in the organic phase by extraction according Folch [45].

In the nuclei the percentage of the total Bi associated with the nuclear membrane fraction was about 1.8 times that the one recovered in the bulk chromatin. Proteins (but not lipids) of the nuclear membranes as well as DNA and histone proteins in the bulk chromatin were identified as targets of the nuclear Bi. The binding of Bi with such targets were not sensitive to dialysis (Table 3) against the same buffer, suggesting Bi was firmly bound to such components.

The soluble matrix was the mitochondrial sub-fraction containing a percentage of radioactivity close to half of the total mitochondrial Bi. The other 50% of the radioactivity was recovered in the heavy and light membranes in a proportion of about 2:1 (Table 4).

In the microsomes, heavy rough and smooth membranes were the sub-fractions with the highest percentage of radioactivity, together retaining 80% of the total microsomal ^{206}Bi (Table 4).

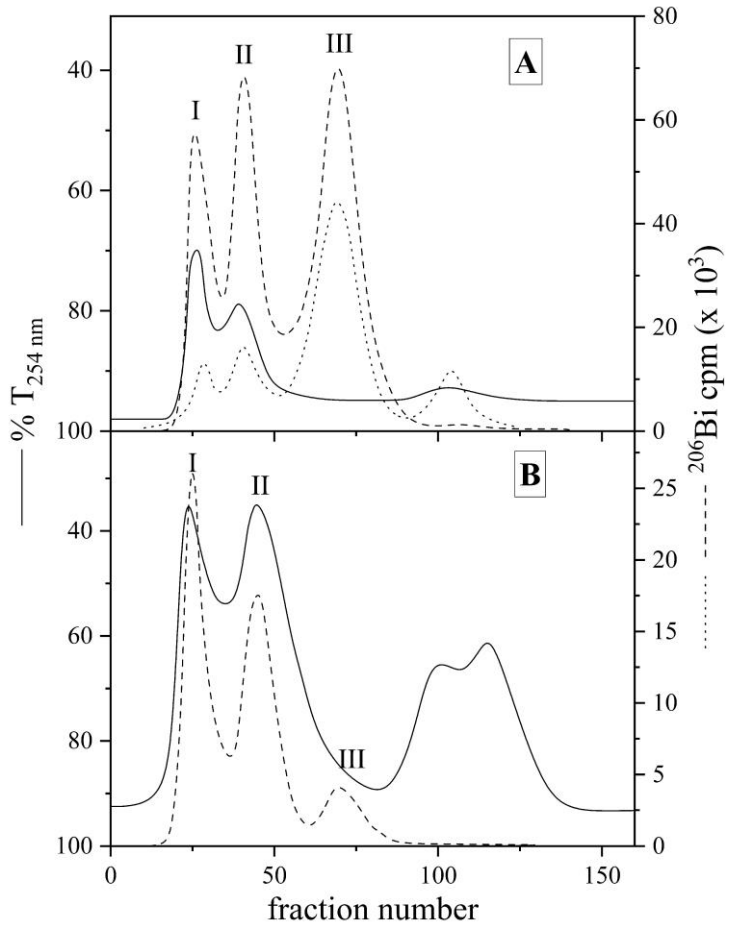

Fig.5 Size exclusion chromatography (SEC) of renal (**A**) and hepatic (**B**) cytosols of rats 24h after i.p. injection of 0.8 µg Bi/kg b.w. as $^{206}Bi(NO)_3$. Aliquots of ^{206}Bi-containing liver or kidney cytosol were absorbed onto Sephadex G-75 column (2.5 cm x 100 cm) previously equilibrated with 10 mM cacodilate buffer, pH 7.2 using the same buffer as eluent.
Molecular weights (MW) were approx. deduced from standard proteins: Albumin, 66 kDa; hen egg ovoalbumin, 45 kDa; bovine pancreas chimotrypsinogen, 25.6 kDa; ribonuclease a, 13.7 kDa. Recovery of ^{206}Bi in the eluate: 89% (liver) and 94.2 % (kidney). The collected fractions were analyzed for the protein content by absorbance at 280 nm and the ^{206}Bi content by integral gamma
The ^{206}Bi profile from SEC of kidney heat- treated cytosol is indicated by ·····.

Fig.5 shows the elution patterns after SEC of the ^{206}Bi-containing hepatic and renal cytosol on Sephadex G-75 resin. In both cases, the ^{206}Bi profiles of the eluate were qualitatively similar, showing three peaks (I, II and III) in regions of the chromatogram with apparent molecular weight of > 300 kDa, 70 kDa and 10 kDa. However, the amount of radioactivity in the three peaks, calculated in percent of the total cytosolic ^{206}Bi, were significantly different ($p< 0.05$) for the liver ^{206}Bi- cytosol compared to that of the corresponding peaks from renal ^{206}Bi- cytosol (48%, 45% and 7% for the liver; 22%, 31% and 47% for the kidney). When SEC on Sephadex G-75 was performed

on the kidney ^{206}Bi-heat-treated cytosol most of the ^{206}Bi of the high molecular weight components (HMWC) and 70 kDa precipitated with the denaturated proteins whereas the ^{206}Bi of the peak (III) at 10 kDa was found substantially stable (Fig.5).

3.4. Dialysis experiments

Less than 13% of Bi was removed from blood and various intracellular components by extensive dialysis against the buffer used in the homogenization and fractionation processes (10 mM cacodylate, pH 7.2) (Table 3). The only exceptions concerned RBC and kidney cytosolic fractions, from which 48.2% and 35.6% of the initial ^{206}Bi in dialysis membrane were respectively removed by dialysis against the cacodylate buffer (Table 3). However, dialysis against acetate buffer at pH 5 or cacodylate buffer pH 7.2 added with complexing agents, particularly DMSA, efficiently removed the radioactivity from all biochemical samples dialyzed.

3.5. Binding of ^{206}Bi to ^{59}Fe-liver ferritin

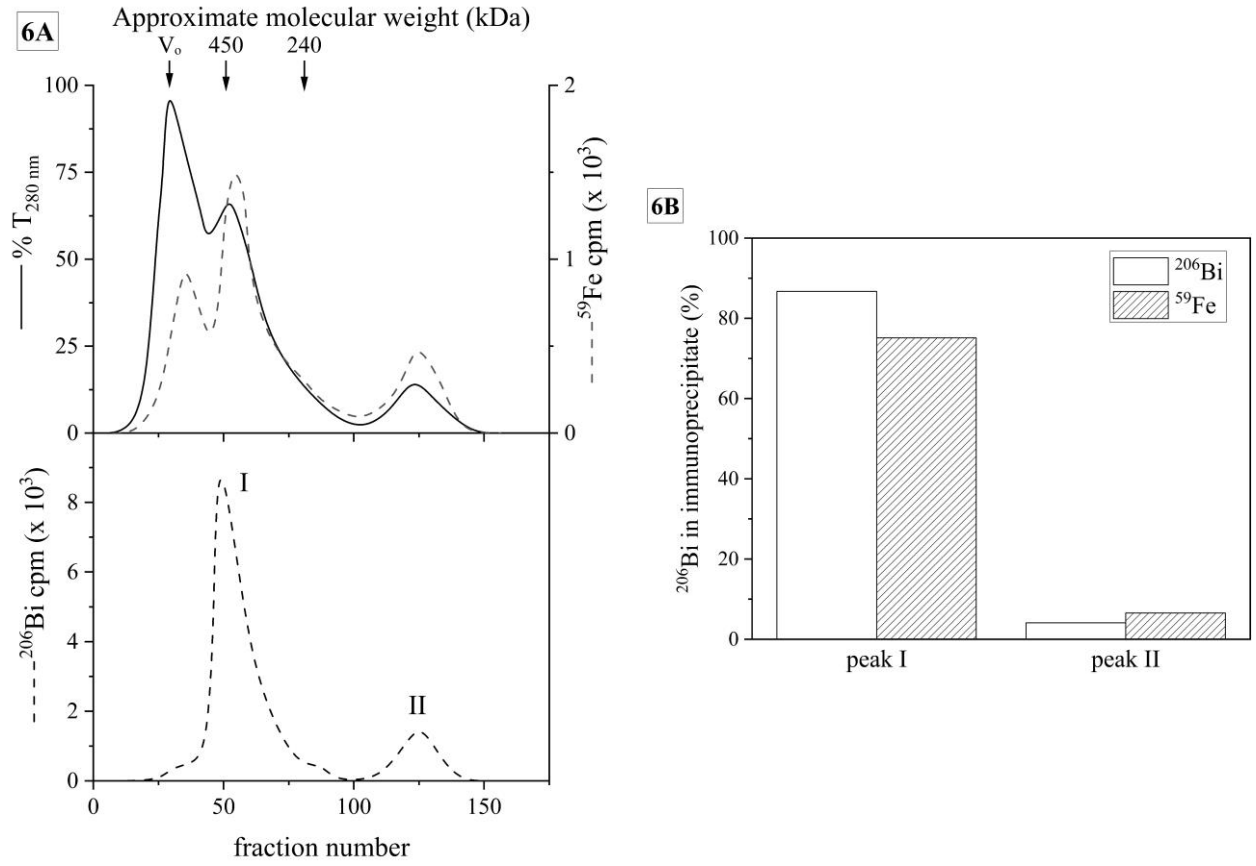

Fig.6 A: SEC on Sepharose 6B of an aliquot of the liver ^{206}Bi+^{59}Fe "heat treated-cytosol" obtained by differential centrifugation. The column (2.5 cm x 60 cm) was previously equilibrated with 10 mM cacodylate buffer, pH 7.2 using the same buffer as eluent. The collected fractions were monitored for proteins at 280 nm, ^{59}Fe and ^{206}Bi content by computer-based high resolution γ-ray spectrometry. Recoveries of ^{206}Bi and ^{59}Fe in the eluate: 79% and 93%, respectively. Molecular weight were approximately deduced from standard proteins: bovine thyroglobulin (669 kDa), horse spleen apoferritin (443 kDa), sweet potato b-amylase (200 kDa), yeast alcohol dehydrogenase (150 kDa), bovine serum albumin (66 kDa), bovine erythrocytes carbonic anhydrase (29 kDa).
B: Percentage of radioactivity immuno-precipitated with ferritin antibody from the pooled ^{206}Bi+^{59}Fe - containing fractions of peaks I and II from SEC on Sepharose 6B (Fig.6A). ^{59}Fe and ^{206}Bi were simultaneously counted in both emerging peaks as well as in the immuno precipitate by computer-based high resolution γ-ray spectrometry. For details see Section 2.7.

Fig.6A shows the SEC on Sepharose 6B of ^{206}Bi+^{59}Fe–"heat treated cytosol" obtained by differential centrifugation of the liver homogenate from the group of rats injected with the two radiotracers (see Section 2.7.). ^{206}Bi emerged from the column at different elution volumes as two peaks, both coincident with as many ^{59}Fe peaks, in the region of apparent molecular weight approximately 450 kDa and 66 kDa. Incubation of the pooled fractions of the two peaks, I and II, with ferritin

antibody shows that only the peak I reacted with specific anti-ferritin. The resulting immunoprecipitate contained 88% of the total ^{206}Bi in that peak together with 74% of the total ^{59}Fe eluted (Fig.6B). Less than 3% of the ^{206}Bi+^{59}Fe –containing peak II reacted with the antibody, suggesting that ^{206}Bi of the peak I was associated to ferritin.

4. Discussion

At present, knowledge on Bi metabolism in laboratory animals refers almost to studies under unnatural “extreme” exposures, i.e. pharmacologically relevant high-doses (up to thousand mg/kg) in relation to its medical use, or infinitesimal-doses (pg/kg as non-carrier-added Bi radioisotopes) for radiobiology protection, diagnostic and radiotherapeutic purposes. No study is reported on metabolic patterns of ultratrace level of Bi (typically µg/kg b.w.) in animal models, being in this context Bi a “heavy metal fallen into oblivion” [1]. The mechanistic understanding of the interaction of Bi with biomolecules at concentrations far below from saturation at the binding site is a key precondition for evaluation of subtle unwanted biochemical induced by ultratrace levels of Bi. Such experimentation poses severe analytical difficulties that may explain the very low quantity of experimental data in literature on the metabolic fate of environmental levels of Bi. We have overcome these difficulties by the cyclotron production of NCA $^{205+206}$Bi radioisotopes that allowed the detection and measurements of pg-fg Bi concentrations in rat tissues, subcellular fractions and molecular components obtained after long and complex separation procedures [51]. Notably, the knowledge of the metabolic fate of ultratrace levels of Bi in mammalian systems is also of growing importance in nanotoxicology research for the safety and sustainable production of nanomaterials. In particular, the enormous potential of Bi-based nanoparticles may be a source of Bi ions in biological fluids whose metabolic fate and subtle toxicity still needs to be

assessed. For this, we have undertaken a study on the biodistribution of ultratrace levels of Bi in the rat. In a previous paper we reported the results of the first part of the study concerned the identification of cellular Bi-binding components in the blood of rats exposed to ultratrace levels of Bi underlying the great caution about any comparison with the bulk of literature, mainly based on "extreme exposure" to Bi have been also discussed [1].

Here we have presented the second part of the same study, namely the one concerning the Bi retention and biodistribution in tissues at intracellular and molecular level.

4.1. Tissue distribution

At 24 h post exposure to 0.8 µgBi/kg b.w. as $^{206}Bi(NO)_3$ kidney was by far the main sequestering tissue of injected Bi, mostly concentrated in the cortex sub-region (Table 1) in agreement with autoradiography observations [52]. This finding is consistent with urinary excretion as primary route of removal of Bi from the body (Fig.1) with biliary or intestinal secretion contributing to fecal excretion [53]. The thymus, spleen, liver, thyroid, trachea, lung, femur, stomach, cerebellum, and duodenum were, in order, the other tissues with declining Bi concentrations. The highest retention of Bi in rat kidney and a similar patterns of Bi in tissues were also reported at high (mg/kg b.w.) and infinitesimal (pg/kg b.w.) dose exposure [54, 55, 56], the uptake being largely independent of the compound administered and the route of exposure [57]. Instead, the significant presence of Bi in thyroid has not been reported elsewhere. Recently, Bi was detected in thyroid of 105 healthy subjects with increasing concentration in the same tissue of patients affected by malignant thyroid tumors [58]. We recovered significant concentrations of Bi in brain and testis (Table 1), suggesting that the element crossed two types of the tightest tissue barriers in mammals, i.e. the blood-brain barrier and blood-testis barrier. However, no perfusion of brain was done so that the presence of Bi in brain could have been a contamination of the element from

blood residue. Assuming a blood residue of 10 µL/g of brain [59] and considering the Bi blood concentration determined (Table 1), we estimated a contamination of the total brain Bi due to residual blood of the order of 1%, confirming that Bi effectively crossed *in vivo* the blood-brain-barrier. This finding is in agreement with observations following acute or subchronic exposure to Bi compounds [55] which suggested that encephalopathy induced by long term treatment with Bi-drugs would be a consequence of a direct interaction of Bi with cellular components of the brain [60]. Moreover, the presence of Bi in cerebellum at higher concentrations than those in the brain may be relevant in relation to the Bi-induced neurotoxic effects [61]. Classic symptoms of ataxia during Bi intoxication suggest the possible cerebellar involvement in Bi encephalopathy [62]. Concerning the crossing of Bi through the blood-testis-barrier an earlier work at very high doses of Bi (500 mg/kg b.w.) as Bi subnitrate, indicated the presence of Bi mainly in Leydig cells of rat testis, pointing at a possible effect of Bi on testicular function and male reproductive capability [63]. Patients with Bi-encephalopathy have also shown bone damage [57]. In our study the presence of Bi in the epiphysis and the concentration gradient in the diaphysis of the femur (Table 1) may suggest bone as potential long-term repository for Bi.

4.2. Subcellular distribution

We investigated the subcellular distribution of Bi in kidney and liver and, for the first time, in spleen, testis and brain (Fig.3). With one exception [55] data on *in vivo* subcellular distribution of Bi are not available in literature. Zidenberg-Cheer's paper [55] reports that after exposure of control rats to NCA $^{205+206}$Bi tracer (pg dosage) kidney and liver nuclear and cytosol fractions had the highest amount of radioactivity. However, only nuclear, mitochondrial and cytosol subcellular fractions were produced by differential centrifugation, so that the degree of cross-contamination due to the ignored fate of lysosome and microsome fractions make the reported results

questionable. Moreover, unlike our work, subcellular fractions were not purified and not tested for their degree of purity by marker enzymes (Table 2, Fig.3).

In the present work, the cytosol from the five tissues analyzed was the fraction with the highest amounts of ^{206}Bi. In addition, similarity of the subcellular repartition pattern in the kidney and spleen was observed when compared with the corresponding liver and testis patterns, being the most evident differences at nuclear and cytosolic level (Fig.3). The remaining radioactivity was distributed between the cellular organelles, being the liver and testis nuclei those with preferential accumulation. However, in the case of purified subcellular fractions of liver using the De Duve's method of presentation (Fig.2) the highest relative specific activity (ratio of the percentage of the total recovered ^{206}Bi, or enzyme, activity in a fraction to the percentage of the total activity recovered in that fraction) was found in the liver lysosomes, followed by nuclei and mitochondria. This finding is relevant in the light of an *in vitro* study in which Bi citrate was taken up by the lysosomes of J774 cells, inducing a lysosomal membrane rupture, a possible up-stream event in apoptosis [64]. In our work, a noteworthy observation comes from the brain subcellular distribution that revealed an affinity of Bi for myelin (Fig.3), a component, surrounding nerve cell axons, containing about 70% of lipids and 30% of proteins [65]. Dialysis experiments provided that Bi was firmly associated to myelin, most likely bound to proteins, being the recovery of the radioactivity in the extracted myelin lipid fraction considered not significant (< 3%) (Fig.3, Table 3)

4.3. Intra-subcellular localization

There are no data on the intrasubcellular distribution of Bi. We investigated this aspect by sub-fractionating the purified liver subcellular fractions (Fig.4, Table 3).

The intranuclear distribution of Bi (Fig.4) showed a marked affinity of the element for nuclear membrane components, excluding a significant association with membrane lipids. However, 35%

of the nuclear Bi penetrated into nuclei where it was associated with intranuclear chromatin components such as DNA and basic histone proteins. Dialysis experiments suggest that such Bi-complexes would involve a stable covalent bond because they were not dissociated during dialysis at physiological pH (Table 3). Previous investigations on the binding of DNA with Bi complexes (Bi(TPC) (TPC= 1,4,7,10-Tetrakis(2-pyridinylmethyl)-1,4,7,10-tetraazacyclododecane) or morin-Bi(III)) were carried out only *in vitro* [66, 67]. In addition, it was suggested that the Bi-histone binding would be ascribed to –SH groups associated with histone molecules [68]. More in general, the sulfur-based biomolecules are considered the primary target for Bi [69], i.e. allowing alcohol dehydrogenase and urease inhibition [70, 71]. However, Brown [72] reported an interaction of Bi with liver nucleoproteins of mice through phosphate and amino groups on histone proteins. In our work, the association of Bi with myelin and DNA suggests that Bi can interact *in vivo* with functional groups other than the sulfhydryl ones.

The intramitochondrial distribution of Bi (Table 4) showed the presence of Bi in all mitochondrial sub-fractions (soluble matrix, outer membranes - light subfraction - and internal membranes - heavy subfraction). Extraction of lipids from the mitochondrial membranes indicated a very low affinity of Bi for lipids (Table 4). This finding suggests that possible effects of Bi on mitochondria may be due to an alteration of membrane permeability or by a binding to reactive groups of mitochondrial proteins or both. *In vivo* distortion of rat mitochondrial inner membranes and *in vitro* inhibition of specific heme pathway enzymes have been reported at high dose exposure to bismuth subnitrate [73].

The intramicrosomal distribution of Bi to smooth and rough surfaced membranes demonstrates the ability of the element to bind ribosomal and membranous components of the endoplasmatic reticulum, not in association, however, with lipid fractions (Table 4). More in general, the associations of Bi with nuclear (Fig.4), mitochondrial and microsomal (Table 4) membranes as well

as brain myelin (Fig.3) suggests that Bi would have a very poor (or no) affinity for lipids, making very doubtful its possible role on lipid metabolism.

The intracytosol Bi localization was investigated by SEC on Sephadex G-150 on liver and kidney ^{206}Bi-containing untreated and heat-treated cytosols. In untreated cytosols three main pools of protein-associated Bi have been identified, in term of molecular size > 300 kDa, 70 kDa and 10 kDa (Fig.5). SEC of heat-treated cytosol suggests that a cysteine thiols-rich metallothionein-like protein (MT) may be the 10 kDa target molecules for Bi, consistent with previous reports [74]. From our study it was not possible to establish whether the binding of Bi with MT is a consequence of the high affinity of the element for the abundant cysteine groups of the protein [75] normally present in the rat liver and kidney (1.6 µg MT/g and 10 µg MT/g tissue, respectively [76]), or if it is a consequence of an ex-novo synthesis of the protein induced by Bi itself, as observed at high exposure doses [77]. Very recently Bi^{3+} salts were proved *in vitro* to bind human apo metallothionein at terminal cysteinal thiolates at pH 7 [78]. Our finding on the consistent binding of Bi to the kidney MT (47% of the cytosol Bi, Fig.5) is in stark contrast to that of Zidenberg-Cherr et al. [55] who did not find any binding of ^{205}Bi with renal MT after injection of NCA ^{205}Bi tracer. However, this finding lacks the reassurance of a satisfactory preparation of the chromatographed renal cytosol whose preparation requires ultracentrifugation of the homogenate at 105 000 g for 110 min [79]. In Zidenberg-Cherr's paper [55] the kidney cytosol was prepared by centrifugation at 17 000 g for 20 min and therefore still containing lysosomes and microsomes.

Interestingly, in rats simultaneously exposed to ^{206}Bi and ^{59}Fe, SEC on Sepharose 6B of the clarified heated [^{206}Bi and ^{59}Fe]-containing liver cytosol followed by immunological precipitation (Fig.6A and Fig.6B) identified ferritin as a target molecule for Bi of the > 300 kDa fraction. This raises the question of whether this Fe-protein may be a component of Bi storage in the liver.

4.4. Dialysis experiments

As a whole the high recoveries (80-95%) of ^{206}Bi from SEC chromatography of ^{206}Bi-containing biocomponents (see legends of Fig.5, Fig.6) showed the ability of Bi to interact strongly with proteins and small biomolecules forming intracellularly complexes. Extensive dialysis of ^{206}Bi-containing intracellular components (Table 3) confirmed this observation, being Bi firmly bound to macromolecules at physiological pH 7.2 with a low degree of their breaking during the applications of the experimental protocols for the isolation of ^{206}Bi-biocomplexes. However, dialysis against an acidic buffer pH 5, or a buffer at constant physiological pH 7.2 with addition of complexing agents resulted in a dissociation of Bi-complexes. Furthermore, we cannot exclude possible weaker noncovalent binding of Bi with cellular biocomponents that could be dissociated during SEC. Other specific methods such as equilibrium dialysis and Hummel and Dreyer techniques [80] would be applied to detect them [1].

5. Conclusions

At the best of our knowledge the present paper represents the first *in vivo* study, on the basis of an environmental toxicology approach [1] aiming at describing retention and binding of Bi in the rat at tissue, intracellular and molecular levels.

Knowledge of metabolic patterns of ultratrace Bi levels is important to assess potential subtle unwanted biochemical changes and for the mechanistic interpretation of toxicological data as exposure determines whether or not, or to which extent, a hazard constitutes a risk. In this context, we are aware that the present study is far from being exhaustive, representing, however, a good basis for continuing the work on key merging aspects: (i) we administered Bi as soluble nitrate. However, it is known that metal speciation plays a key role in determining metabolism and biochemical effects of heavy metals [51]. We know too little about the concentrations of Bi in food

[81] and we ignore its chemical-physical form(s) to which humans are daily exposed. More work in this area is awaited; (ii) we considered a single short exposure time. Biokinetic investigations are needed in order to identify tissue and Bi-binding components responsible for long term retention of the element, i.e. bone and kidney metallothionein-like (MT) proteins; (iv) we have shown the *in vivo* formation of Bi complexes with non-heme non-enzymatic Fe-containing proteins (transferrin [1] and in the present paper ferritin). Relationships between Bi and Fe metabolism (i.e. interaction with Fe heme-containing proteins) need to be deepened; (v) we recommend cytotoxicity and mechanistic studies on the interaction of Bi with biocomponents for the first time identified as Bi binders of tissues (i.e. thyroid), intra-subcellular components (i.e. nuclear, mitochondrial, microsomal membranes) and individual biomolecules (i.e. transferrin, ferritin, myelin, DNA, MT). This would be conveniently studied *in vitro* by cell cultures and isolated individual biocomponents. This paper is of interest not only in improving the understanding of the *in vivo* metabolic fate of ultratrace levels of Bi and its mechanism of action but also in providing a basis for the design of more effective Bi-based agents in health care.

Contributorship

Sabbioni: Conceptualization, Writing - Original draft, Resources, Supervision, Investigation

Groppi: Investigation, Funding acquisition

Di Gioacchino: Writing - Review & Editing, Supervision

Petrarca: Writing Review & Editing, Visualization

Manenti: Investigation, Formal analysis, Visualization, Writing - Review & Editing

Declaration of Competing Interest

The authors declare that they have no conflicts of interest.

Acknowledgment

We are grateful to Mrs. J.Edel for the excellent technical assistance with the work of laboratory animals and gel filtration experiments. We would also like to thank Messrs R.Pietra and G. Tettamanti (Ascom, Milan) for the assistance with radioactive counting by γ-ray spectrometry. Special thanks to Dott. Lorenzo Vilona for his contribution in reviewing the English language of the manuscript.

References

1. Sabbioni E., Groppi F., Di Gioacchino G., Petrarca C., Manenti S. Metallobiochemistry of ultratrace levels of bismuth in the rat - I. Metabolic patterns of $^{205+206}Bi^{3+}$ in the blood. Journal of Trace Elements in Medicine and Biology, 2020, Submitted Paper

2. Marcillac P., Coron N., Dambier G., LeBlanc J., Moalic J.P. (2003). Experimental Detection of α-Particles from the Radioactive Decay of Natural Bismuth. Nature. 422. 876-8. 10.1038/nature01541.

3. Ayodele Temidayo Odularu, "Bismuth as Smart Material and Its Application in the Ninth Principle of Sustainable Chemistry", Journal of Chemistry, vol. 2020, Article ID 9802934, 15 pages, 2020. https://doi.org/10.1155/2020/9802934

4. Wang R, Li H, Sun H. Bismuth: Environmental Pollution and Health Effects. Encyclopedia of Environmental Health. 2019;415-423. doi:10.1016/B978-0-12-409548-9.11870-6

5. Meng, Xiangchao & Zhang, Zisheng. (2016). Bismuth-based Photocatalytic Semiconductors: Introduction, Challenges and Possible Approaches. Journal of Molecular Catalysis A: Chemical. 423. 10.1016/j.molcata.2016.07.030.

6. Yang N, Sun H. Bismuth: Environmental Pollution and Health Effects. Encyclopedia of Environmental Health. 2011;414-420. doi:10.1016/B978-0-444-52272-6.00374-3

7. Kang, S., Kim, J., Pyo, J. et al. Design of Magnetic Force Field for Trajectory Control of Levitated Diamagnetic Graphite. Int. J. of Precis. Eng. and Manuf.-Green Tech. 5, 341–347 (2018). https://doi.org/10.1007/s40684-018-0036-3

8. European Commission, SCCS/1499/12 (Scientific Committee on Consumer Safety), Opinion on bismuth citrate, 12 December 2013 Doi: 10.2772/74214

9. Patty-Beliles, R.P. The metals: Bismuth. In Patty's Industrial Hygiene and Toxicology, 4th ed.; Clayton, G.D., Clayton, F.E., Eds.; John Wiley & Sons: New York, NY, USA, 1994; Volume 2, pp. 1948–1954.

10. Sun H., Li H., Sadler P. J. (1997). The Biological and Medicinal Chemistry of Bismuth. Chemische Berichte, 130(6), 669–681. doi:10.1002/cber.19971300602

11. Schindler R., Heemann U., Haug U., Stoelck B., Karatas A., Pohle C., Deppisch R., Beck W., Hollenbeck M. (2010). Bismuth coating of non-tunneled haemodialysis catheters reduces bacterial colonization: A randomized controlled trial. Nephrology, dialysis, transplantation: official publication of the European Dialysis and Transplant Association - European Renal Association. 25. 2651-6. 10.1093/ndt/gfq052.

12. Mohan, R. Green bismuth. Nature Chem 2, 336 (2010). https://doi.org/10.1038/nchem.609

13. Cengiz, N., Uslu, Y., Gök, F. et al. Acute renal failure after overdose of colloidal bismuth subcitrate. Pediatr Nephrol 20, 1355–1358 (2005). https://doi.org/10.1007/s00467-005-1993-7

14. Borovikova, L. & Polyakova, I. & Korotkikh, E. & Lavrent'ev, V. & Kipper, A. & Pisarev, O. (2018). Synthesis and Stabilization of Bismuth Nanoparticles in Aqueous Solutions. Russian Journal of Physical Chemistry. 92 (2018). 2253-2256. 10.1134/S0036024418110055.

15. William W. Anku, Samuel O.B. Oppong and Penny P. Govender (2018). Bismuth-Based Nanoparticles as Photocatalytic Materials, In: Bismuth - Advanced Applications and Defects Characterization, Ying Zhou, Fan Dong and Shengming Jin, IntechOpen, DOI: 10.5772/intechopen.75104.

16. M. Shahbazi, L. Faghfouri, M. P. A. Ferreira, P. Figueiredo, H. Maleki, F. Sefat, J. Hirvonen and H. A. Santos, The versatile biomedical applications of bismuth-based nanoparticles and composites: therapeutic, diagnostic, biosensing, and regenerative propertiesChem. Soc. Rev., 2020, 49, 1253 DOI: 10.1039/C9CS00283A

17. Negar Motakef-Kazemi and Masoumeh Yaqoubi Green Synthesis and Characterization of Bismuth Oxide Nanoparticle Using Mentha Pulegium Extract. Iranian Journal of Pharmaceutical Research (2020), 19 (2): 70-79 DOI: 10.22037/ijpr.2019.15578.13190R.

18. AR Badireddy, R. Hernandez-Delgadillo, R. I. Sánchez-Nájera, S. Chellam, and C. Cabral-Romero, "Synthesis and characterization of lipophilic bismuth dimercaptopropanol nanoparticles and their effects on oral microorganisms growth and biofilm formation," Journal of Nanoparticle Research, vol. 16, no. 6, article 2456, 2014.

19. Rodríguez-Luis, Osvelia & Hernandez-Delgadillo, Rene & Pineda-Aguilar, Nayely & Vargas-Villarreal, Javier & Gonzalez-Salazar, Francisco & Garza-González, Jesús & Hernández-García, Magda & Chellam, Shankar & Cabral-Romero, Claudio. (2017). Effect of Bismuth Lipophilic Nanoparticles (BisBAL NPs) on Trichomonas vaginalis Growth. Journal of Nanoscience and Nanotechnology. 17. 4618-4622. 10.1166/jnn.2017.13743.

20. Vazquez Muñoz, Roberto & Arellano-Jimenez, Maria Josefina & Lopez-Ribot, Jose. (2020). Bismuth nanoparticles obtained by a facile synthesis method exhibit antimicrobial activity against Staphylococcus aureus and Candida albicans. 10.1101/2020.06.05.137109.

21. Li, Z., Hu, Y., Howard, K. A., Jiang, T., Fan, X., Miao, Z., Sun, Y., Besenbacher, F. and Yu, M. (2016) 'Multifunctional Bismuth Selenide Nanocomposites for Antitumor Thermo-Chemotherapy and Imaging', ACS Nano, 10(1), pp. 984-97.

22. Liu, Y., Zhuang, J., Zhang, X., Yue, C., Zhu, N., Yang, L., Wang, Y., Chen, T. and Zhang, L. W. (2017) 'Autophagy associated cytotoxicity and cellular uptake mechanisms of bismuth nanoparticles in human kidney cells', Toxicol Lett, 275, pp. 39-48

23. Stewart, C., Konstantinov, K., McKinnon, S., Guatelli, S., Lerch, M., Rosenfeld, A., Tehei, M. and Corde, S. (2016) 'First proof of bismuth oxide nanoparticles as efficient radiosensitisers on highly radioresistant cancer cells', Phys Med, 32(11), pp. 1444-1452

24. Khan, I., Saeed, K., & Khan, I. (2017). Nanoparticles: Properties, applications and toxicities. Arabian Journal of Chemistry. doi:10.1016/j.arabjc.2017.05.011

25. Abudayyak, M., Öztaş, E., Arici, M. and Özhan, G. (2017) 'Investigation of the toxicity of bismuth oxide nanoparticles in various cell lines', Chemosphere, 169, pp. 117-123.

26. Wei B., Zhang X., Zhang C., Jiang Y., Fu Y.Y., Yu C., Sun S.K., Yan X.P., 2016, Facile synthesis of uniform- sized bismuth nanoparticles for CT visualization of gastrointestinal tract in vivo, ACS Applied Materials and Interfaces, 8, 12720-12726.

27. Hernandez-Delgadillo, Rene; Badireddy, Appala Raju; Zaragoza-Magaña, Valentin; Sánchez-Nájera, Rosa Isela; Chellam, Shankararaman; Cabral-Romero, Claudio (2015). Effect of Lipophilic Bismuth Nanoparticles on Erythrocytes. Journal of Nanomaterials.

28. Reus TL, Machado TN, Bezerra AG Jr, Marcon BH, Paschoal ACC, Kuligovski C, de Aguiar AM, Dallagiovanna B. Dose-dependent cytotoxicity of bismuth nanoparticles produced by LASiS in a reference mammalian cell line BALB/c 3T3. Toxicol In Vitro. 2018 53:99-106. doi: 10.1016/j.tiv.2018.07.003

29. Mishra, V., Baranwal, V., Mishra, R.K. et al. Immunotoxicological impact and biodistribution assessment of bismuth selenide (Bi_2Se_3) nanoparticles following intratracheal instillation in mice. Sci Rep 7, 18032 (2017). https://doi.org/10.1038/s41598-017-18126-y

30. Stephens, L. J., Munuganti, S., Duffin, R. N., Werrett, M. V., & Andrews, P. C. (2020). Is Bismuth Really the “Green” Metal? Exploring the Antimicrobial Activity and Cytotoxicity of Organobismuth Thiolate Complexes. Inorganic Chemistry. Doi:10.1021/acs.inorgchem.9b03550

31. Sabbioni E, Fortaner S, Farina M, Del Torchio R, Olivato I, Petrarca C, Bernardini G, Mariani-Costantini R, Perconti S, Di Giampaolo L, Gornati R, Di Gioacchino M. Cytotoxicity and morphological transforming potential of cobalt nanoparticles, microparticles and ions in Balb/3T3 mouse fibroblasts: an in vitro model. Nanotoxicology. 2014 Jun;8(4):455-64. Doi: 10.3109/17435390.2013.796538. Epub 2013 May 15. PMID: 23586465.

32. EU, Directive 86/609/EEC of 24 November 1986 on the approximation of laws, regulations and administrative provisions of the Member States regarding the protection of animals used for experimental and other scientific purposes. Official Journal of the European Community L358 (1986) 1-29.

33. Heydorn WE, Joseph Creed G, Patel J, Jacobowitz DM. Distribution of proteins in different subcellular fractions of rat brain studied by two-dimensional gel electrophoresis. Neurochemistry International. 9: 357-70. PMID 20493135 DOI: 10.1016/0197-0186(86)90077-X

34. Franke W.W., Barbara Deumling , H. Zentgraf , H. Falk , P.M.M. Raex , Experimental Cell ResearchNuclear membranes from mammalian liver: IV. Characterization of membrane-attached DNA Experimental Cell Research Experimental Cell Research Volume 81, Issue 2, October 1973, Pages 365-392 https://doi.org/10.1016/0014-4827(73)90527-2

35. Sottocasa GL, Kuylenstierna B, Ernster L, Bergstrand A. An electron-transport system associated with the outer membrane of liver mitochondria. A biochemical and morphological study. J Cell Biol. 1967;32(2):415-438. doi:10.1083/jcb.32.2.415

36. K. Burton, A study of the conditions and mechanism of the diphenylamine reaction for the colorimetric estimation of deoxyribonucleic acid Biochem. J. 62, 315 (1956).

37. SJ Cooperstein and A. Lazarow, A microspectrophotometric method for the determination of cytochrome oxidase. J. Biol. Chem. 189, 665-670 (1951)

38. K. Dodgson, B. Spencer, J. Thomas, Studies on sulphatases 9. The arylsulphatases of mammalian livers. Biochem. J. 59, 29-37 (1955).

39. L. C. Eriksson, Studies on the biogenesis of endoplasmic reticulum and in the liver cell. 1973 Acta Pathol Microbial. &and. Suppl.239:1

40. Vassault A. 1983. Lactate dehydrogenase. In: Bergmeyer HU, Bergmeyer J, Graßl M, editors. Methods of enzymatic analysis: Enzymes I oxidoreductases, transferases. Vol. 3. Basel: Verlag Chemie. p 118 – 126

41. Bradford and sensitive method for the quantitation of microgram quantities of protein utilizing the principle of protein-dye binding. Anal Biochem. 1976;72:248-254. doi:10.1006/abio.1976.9999

42. De Duve C, PRESSMAN BC, GIANETTO R, WATTIAUX R, APPELMANS F. Tissue fractionation studies. 6. Intracellular distribution patterns of enzymes in rat-liver tissue. Biochem J. 1955;60(4):604-617

43. Tata JR, Recommended methods for the isolation of microsomes and submicrosomal fraction in subcellular components, in Subcellular components. Preparation and fractionation, GD Birnie ed, Butterworth, London, chapter 8, pp.185-213

44. Sabbioni E, Fortaner S, Bosisio S, et al. Metabolic fate of ultratrace levels of GeCl(4) in the rat and in vitro studies on its basal cytotoxicity and carcinogenic potential in Balb/3T3 and HaCaT cell lines dagger. J Appl Toxicol. 2010;30(1):34-41. doi:10.1002/jat.1469

45. Folch J, Lees M, Stanley GHS. A simple method for the isolation and purification of total lipides from animal tissues. J Biol Chem. 1957;226(1):497–50 https://doi.org/10.1007/978-94-007-7864-1_89-1

46. Millar JA, Cumming RL, Smith JA, Goldberg A. Effect of actinomycin D, cycloheximide, and acute blood loss of ferritin synthesis in rat liver. Biochem J. 1970;119(4):643-649. doi:10.1042/bj1190643

47. Abraham Mazur, Saul Green, and A. Carleton Mechanism of Plasma Iron Incorporation into Hepatic Ferritin J. Biol. Chem. 1960 235: 595-603

48. Caster WO, PONCELET J, SIMON AB, ARMSTRONG WD. Tissue weights of the rat. I. Normal values determined by dissection and chemical methods. Proc Soc Exp Biol Med. 1956;91(1):122-126. doi:10.3181/00379727-91-22186

49. Schoeffner DJ, Warren DA, Muralidara S, Bruckner JV, Simmons JE. Organ weights and fat volume in rats as a function of strain and age. J Toxicol Environ Health A. 1999;56(7):449-462. doi:10.1080/009841099157917

50. V. R. YOUNG, The role of skeletal In of and cardiac metabolism. regulation Ed.), Vol. 4, protein pp. 585-728. Academic Mammalian Protein Metabolism (H. N. Munro, New Press, 1970. York/London

51. Sabbioni, E., Di Gioacchino, M., Farina, M., Groppi, F., Manenti, S., Radioanalytical and nuclear techniques in trace metal toxicology research. J Radioanal Nucl Chem 318, 1749–1763 (2018). https://doi.org/10.1007/s10967-018-6321-3

52. Russ GA, Bigler RE, Tilbury RS, Woodard HQ, Laughlin JS. Metabolic studies with radiobismuth. I. Retention and distribution of 206Bi in the normal rat. Radiat Res. 1975;63(3):443-454

53. Maria A. Luppino and Allan J. McLeanPlasma and tissue distribution of bismuth in normal and cirrhotic rats Analyst, 1995,120, 883-886

54. Lee SP, Lim TH, Pybus J, Clarke AC. Tissue distribution of orally administered bismuth in the rat. Clin Exp Pharmacol Physiol. 1980;7(3):319-324. doi:10.1111/j.1440-1681.1980.tb00076.x

55. Zidenberg-Cherr S, Parks NJ, Keen CL. Tissue and subcellular distribution of bismuth radiotracer in the rat: considerations of cytotoxicity and microdosimetry for bismuth radiopharmaceuticals. Radiat Res. 1987;111(1):119-129.

56. Rao N, Feldman S. Disposition of bismuth in the rat. I. Red blood cell and plasma protein binding. Pharm Res. 1990;7(2):188-191. doi:10.1023/a:1015841105215

57. Slikkerveer A, de Wolff FA.Pharmacokinetics and toxicity of bismuth compounds. In: Slikkerveer A ed. Bismuth: biokinetics, toxicity and experimental therapy of overdosage Netherlands: Leiden University, 1992

58. Vladimir Zaichick and Sofia Zaichick. “Fifty Trace Element Contents in Normal and Cancerous Thyroid”. Acta Scientific Cancer Biology 2.8 (2018): 21-38

59. Cremer JE, Seville MP. Regional brain blood flow, blood volume, and haematocrit values in the adult rat. J Cereb Blood Flow Metab. 1983;3(2):254-256. doi:10.1038/jcbfm.1983.35

60. Lechat P, Palliere M, Gernez G, Dechy H, Letteron N. Repartition comparee du bismuth dans I'organisme du rat apres administration orale repetee de different sels. Annales Pharmaceutiques Francaises 34: 179-182, 1976

61. Bruinink A, Reiser P, Müller M, Gähwiler BH, Zbinden G. Neurotoxic effects of bismuth in vitro. Toxicology in Vitro : an International Journal Published in Association with BIBRA. 1992 Jul;6(4):285-293. DOI: 10.1016/0887-2333(92)90018-m

62. Larsen A, Stoltenberg M, West MJ, Danscher G. Influence of bismuth on the number of neurons in cerebellum and hippocampus of normal and hypoxia-exposed mouse brain: a stereological study. J Appl Toxicol. 2005;25(5):383-392. doi:10.1002/jat.1061

63. M Stoltenberg a, G Danscher a, R Pamphlett b, M.M Christensen a, J Rungby a Histochemical tracing of bismuth in testis from rats exposed intraperitoneally to bismuth subnitrate Reproductive ToxicologyVolume 14, Issue 1, January–February 2000, Pages 65-71 https://doi.org/10.1016/S0890-6238(99)00060-X

64. Stoltenberg M, Larsen A, Zhao M, Danscher G, Brunk UT. Bismuth-induced lysosomal rupture in J774 cells. APMIS. 2002 May;110(5):396-402. doi: 10.1034/j.1600-0463.2002.100505.x. PMID: 12076257.

65. Morell P, Quarles RH. Characteristic Composition of Myelin. In: Siegel GJ, Agranoff BW, Albers RW, et al., editors. Basic Neurochemistry: Molecular, Cellular and Medical Aspects.

6th edition. Philadelphia: Lippincott-Raven; 1999. Available from: https://www.ncbi.nlm.nih.gov/books/NBK28221

66. Xiaoyong Wang, Xianming Zhang, Jun Lin, Jingwen Chen, Qiang Xu and Zijian Guo DNA-binding property and antitumor activity of bismuth(iii) complex with 1,4,7,10-tetrakis(2-pyridylmethyl)-1,4,7,10-tetraazacyclododecane† Dalton Trans., 2003, 2379-2380

67. ENSAFI, Ali A.; HAJIAN, Reza and EBRAHIMI, Sara. Study on the interaction between morin-bi(III) complex and DNA with the use of methylene blue dye as a fluorophor probe. J. Braz. Chem. Soc. [online]. 2009, vol.20, n.2 [cited 2020-07-11], pp.266-276.doi.org/10.1590/S0103-50532009000200011

68. M.A. Hayat in Stains and Cytochemical Methods, Springer Science & Business Media, 1993 ISBN 0306442949, 9780306442940

69. Chaleil D, Lefevre F, Allain P, Martin GJ Enhanced bismuth digestive absorption in rats by some sulfhydry compounds: NMR study of complexes formed J Inorg Biochem 1981; 15: 213-21.

70. Jin L, Szeto KY, Zhang L, Du W, Sun H. Inhibition of alcohol dehydrogenase by bismuth. J Inorg Biochem. 2004;98(8):1331-1337. doi:10.1016/j.jinorgbio.2004.03.016

71. Zhang, L., Mulrooney, S.B., Leung, A.F.K. et al. Inhibition of urease by bismuth(III): Implications for the mechanism of action of bismuth drugs. Biometals 19, 503–511 (2006). https://doi.org/10.1007/s10534-005-5449-0

72. Brown GL, Locke M. Nucleoprotein localization by bismuth staining. Tissue Cell. 1978;10(2):365-388. doi:10.1016/0040-8166(78)90030-7

73. Woods JS, Fowler BA. Alteration of mitochondrial structure and heme biosynthetic parameters in liver and kidney cells by bismuth. Toxicol Appl Pharmacol. 1987;90(2):274-283. doi:10.1016/0041-008x(87)90335-8

74. Szymańska JA, Piotrowski JK. Studies to identify the low molecular weight bismuth-binding proteins in rat kidney. Biochem Pharmacol. 1980;29(21):2913-2918. doi:10.1016/0006-2952(80)90036-2

75. Sabolić, I., Breljak, D., Škarica, M. et al. Role of metallothionein in cadmium traffic and toxicity in kidneys and other mammalian organs. Biometals 23, 897–926 (2010). https://doi.org/10.1007/s10534-010-9351-z

76. Eaton, ICRP, 2017. Occupational intakes of radionuclides: Part 3. ICRP Publication 137. Ann. ICRP 46(3/4).

77. J. K. Piotrowski & Jadwiga A. Szymańska (1976) Influence of certain metals on the level of metallothionein-like proteins in the liver and kidneys of rats, Journal of Toxicology and Environmental Health: Current Issues, 1:6, 991-1002, DOI: 10.1080/15287397609529402

78. Korkola, N. C.; Scarrow, P. M. & Stillman, M. J. pH dependence of the non-cooperative binding of Bi^{3+} to human apo-metallothionein 1A: kinetics, speciation, and stoichiometry Metallomics, The Royal Society of Chemistry, 2020, 12, 435-448

79. Hogeboom GH. [3] Fractionation of cell components of animal tissues Methods in Enzymology. 1: 16-19. DOI: 10.1016/0076-6879(55)01007-0

80. Berger G, Girault G. Macromolecule-ligand binding studied by the Hummel and Dreyer method: current state of the methodology. J Chromatogr B Analyt Technol Biomed Life Sci. 2003;797(1-2):51-61. doi:10.1016/s1570-0232(03)00482-3

81. Ruiz-de-Cenzano M, Rochina-Marco A, Cervera ML, de la Guardia M. Evaluation of the Content of Antimony, Arsenic, Bismuth, Selenium, Tellurium and Their Inorganic Forms in Commercially Baby Foods. Biol Trace Elem Res. 2017 Dec;180(2):355-365. doi: 10.1007/s12011-017-1018-y. Epub 2017